Introduction to indoor networking concepts and challenges in LiFi

HARALD HAAS,* Ⓘ LIANG YIN, CHENG CHEN, STEFAN VIDEV, DAMIAN PAROL,
ENRIQUE POVES, HAMADA ALSHAER, AND MOHAMED SUFYAN ISLIM Ⓘ

*Institute for Digital Communications, School of Engineering, The University of Edinburgh, LiFi Research and Development Centre, EH9 3JL,
Edinburgh, UK*
Corresponding author: h.haas@ed.ac.uk

LiFi is networked, bidirectional wireless communication with light. It is used to connect fixed and mobile devices at very high data rates by harnessing the visible light and infrared spectrum. Combined, these spectral resources are 2600 times larger than the entire radio frequency (RF) spectrum. This paper provides the motivation behind why LiFi is a very timely technology, especially for 6th generation (6G) cellular communications. It discusses and reviews essential networking technologies, such as interference mitigation and hybrid LiFi/Wi-Fi networking topologies. We also consider the seamless integration of LiFi into existing wireless networks to form heterogeneous networks across the optical and RF domains and discuss implications and solutions in terms of load balancing. Finally, we provide the results of a real-world hybrid LiFi/Wi-Fi network deployment in a software defined networking testbed. In addition, results from a LiFi deployment in a school classroom are provided, which show that Wi-Fi network performance can be improved significantly by offloading traffic to the LiFi.   © 2019 Optical Society of America

https://doi.org/10.1364/JOCN.12.00A190

1. INTRODUCTION: A HISTORICAL PERSPECTIVE

Before Alexander Graham Bell invented the telephone, he had already demonstrated the photophone where he used sunlight to transmit voice over more than 200 m in 1880. Sunlight was reflected by a vibrating mirror, which was connected to a microphone. At the receiver, a parabolic mirror with a selenium cell in the center captured the intensity variations of the reflected light and converted them into an electrical signal that was connected to a loudspeaker. The intensity variations were proportional to the fluctuating current generated by the microphone, so he was able to transmit analog voice signals wirelessly using sunlight. About 20 years later the era of light emitting diodes (LEDs) started [1], and 100 years later researchers developed the first wireless data communication systems based on artificial light using LEDs—predominately at Bell Labs [2] and IBM Research labs [3]. Researchers at IBM developed the first networked infrared-light-based wireless networks as interconnects between distributed computers in the 1980s [3]. Barry [4,5] laid the theoretical foundations of indoor communication with infrared LEDs. In the meantime, huge efforts had begun to develop the blue LED after Holonyak invented the first LED emitting in the visible light spectrum (red) in 1962 [6]. However, it took 31 years until Nakamura and colleagues were able to demonstrate the first blue LED [7,8].

This was the final piece of the jigsaw toward the white LED, a development that drastically changed the application landscape of LEDs from mere signaling devices to illumination devices, replacing the highly energy-inefficient incandescent light bulb. Bell's vision to use light for wireless communications, but now artificial white light for digital wireless communication and at very high transmission speeds, moved significantly closer to reality. Nakagawa and colleagues at the Visible Light Communication Consortium (VLCC) started to use white high-brightness LEDs for data communications around the year 2000. They referred to it as visible light communication (VLC) [9] and concentrated their research efforts on application studies [10]. Other research in this area focused on the development of new techniques to enhance the data rates of the bandlimited phosphor-coated white LEDs [11], and the first experimental results on the exploitation of the high crest factor of orthogonal frequency division multiplexing (OFDM) for intensity modulation/direct detection (IM/DD) were reported in [12]. A different class of free-space light communication is optical camera communication (OCC), which uses embedded camera sensors as receivers [13–15]. OCC is typically one-way (simplex) communication with the main use case being indoor positioning and navigation [16–19]. LiFi is a special form of VLC and describes an entire wireless network, which supports
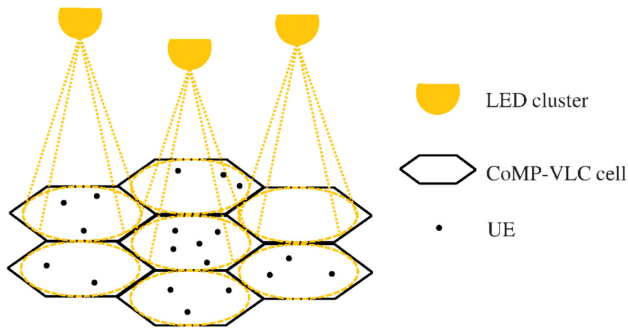
Fig. 1. Here we illustrate a LiFi network. Each light acts as an optical access point, which serves multiple user equipment within its illumination area/cell. Users can also move, and they will be served by different light bulbs as they roam. This change of serving access point happens seamlessly. Several cells form a cluster, UEs at the cell edges can be served by multiple access points to avoid interference. This technique is referred to as cooperative multipoint (CoMP) transmission.

user mobility, handover, and multiuser access, and is part of the existing heterogeneous wireless networks [20] (see Fig. 1).

This LiFi network is also referred to as an optical attocell network [21]. An optical attocell network aims to address the looming spectrum crisis in radio frequency (RF) communications [22] where the important metric is not link data rate but data density. This is defined as the bits per second per unit area. It was shown that a LiFi network can increase the data density by three orders of magnitude while completely avoiding interference with existing RF-based networks [23]. This means that the LiFi network simply adds capacity to the existing RF networks. Most importantly, it can use the existing lighting infrastructure. From a lighting industry perspective, this development has been welcomed because the 20–30 year lifetime of an LED light bulb means that business models inevitably have to move from sales of lighting devices to services, and light-as-a-service (LaaS) has become a dominating business theme in the lighting industry. The LiFi network exploits the lighting system and turns lighting into a wireless communication network that potentially enables hundreds of services.

There has been notable progress in the commercialization of LiFi technology. An important factor is the ongoing development of a standard within the IEEE 802.11bb Task Group [24]. The target date for a first standard release is 2021. This new standard will ensure seamless integration of LiFi into the existing wireless standards. Furthermore, discussions on 6th generation (6G) technologies have started. There is a view that new spectrum is required, which has put VLC and LiFi on the map for 6G [25].

Contributions:

1. This paper surveys networking techniques for LiFi. The major body of literature in VLC is on physical layer techniques, primarily modulation techniques, in conjunction with experimental point-to-point communication links in an ideal lab-bench environment. The VLC links are mostly perfectly aligned. In a LiFi network that supports user mobility and random orientations of mobile terminals these assumptions no longer hold. In addition, because there are multiple simultaneously active links in a network, interference degrades link performance. However, the characteristic of interference is different from RF networks. This paper comprehensively reviews techniques that have dealt with these issues. It demonstrates how LiFi can uniquely improve wireless networking performance. The paper specifically showcases that LiFi can advance area spectral efficiency by means of cell densification in a way that it is not easily possible in RF.

2. The paper provides novel experimental results from a hybrid LiFi/Wi-Fi networking testbed, which has been developed as part of the project TOUCAN (Towards Ultimate Convergence of All Networks) in the United Kingdom.

3. The paper provides for the first time, to the best or our knowledge, experimental results of a real-world hybrid LiFi/Wi-Fi deployment in a school in Scotland. These results highlight the benefits of integrated LiFi networks that stem from their data traffic offload capabilities.

We believe all these contributions are novel and distinct from existing literature on LiFi networking and VLC. The experimental networking results in this paper provide novel insights into key areas that could be optimized to improve wireless networking performance. We also note that other light communication technologies, such as OCC, free-space optical, and more general VLC, are not the focus of this paper, and the interested reader is referred to a recent survey on the wider topic of optical wireless communications [26].

Section 2 summarizes channel models. The basic concept and the challenges of LiFi networks are introduced in Section 3. Interference mitigation approaches are discussed in Section 4. Section 5 provides insights into the capacity of LiFi networks based on different network deployments. It showcases results stemming from a hybrid LiFi/Wi-Fi testbed. Lastly, it reports measurement results from a real-world hybrid LiFi/Wi-Fi network deployment in a school. Section 6 concludes the paper.

2. CHANNEL MODELS IN VLC AND LIFI

One of the most important factors that determines the performance of VLC transmission systems and LiFi networks is the quality of the communication channel. In an incoherent IM/DD optical system, the transmission channel is typically composed of two parts. One part is related to the filtering of front-end elements, and the second part is related to indoor free-space propagation [27], as shown in Fig. 2(a). Regarding the latter, there is a large body of literature for infrared channel models [28,29], but there are only a few studies on visible light channel models. In [30] it is shown that some materials exhibit fundamentally different reflection properties in the visible light spectrum compared to the infrared spectrum. The work showcases the impact of these differences on the channel model. Following on from this, Uysal has developed VLC reference channel models for the IEEE 802.11bb task group on light communication [31].
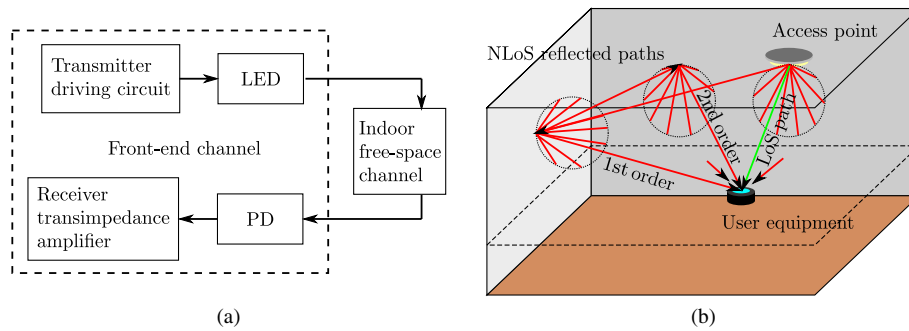
Fig. 2.   (a) LiFi channel block diagram. (b) Illustration of the indoor free-space VLC channel.

A. Impact of Optical Front-Ends on VLC and LiFi Channels

The typical optical front-ends for incoherent IM/DD optical wireless systems include LEDs at the transmitter and photodiodes (PDs) at the receiver. In addition, for the design of practical systems, the effects of front-end electronics, such as LED drivers at the transmitter and optics as well as transimpedance amplifiers at the receiver, should be included in the channel model; see Fig. 2(a). These devices exhibit low-pass characteristics, which can limit maximum achievable data rates. The front-end channel of a specified VLC system can be obtained experimentally by measuring the channel response of a short-range point-to-point link [32]. The exact transfer function depends on the actual devices. Therefore, it is very difficult to characterize this element of the channel by generic models, until good parametrized models become available. This requires more research. Many researchers have tried to use simple models using curve-fitting techniques to approximate the characteristics of the front-end channel [27,33,34]. This approach shows acceptable accuracy compared to measured results but is very time consuming and renders comparative studies difficult. Most of the existing studies on the optical wireless channel consider a Lambertian radiation pattern because it is simple to use and widely accepted by the VLC research community. However, a number of studies [35,36] have shown that some LED lamps in practice produce radiation patterns that are very different from the Lambertian model. Moreover, these studies have shown that the channel characteristics in terms of path loss and root mean square delay spread are highly dependent on the LED radiation pattern.

B. Impact of Indoor Free-Space Light Propagation on VLC and LiFi Channels

Optical signals experience considerable attenuation when they travel in free space. In addition, the signal components arrive at the detector via different paths, including physical effects, such as reflection and scattering [37,38]. These effects cause different time delays for the arriving signals, thereby leading to unique channel power delay profiles. The primary channel component in free-space light propagation is the transmission via a line-of-sight (LoS) path, as shown in Fig. 2(b), which can be characterized by a simple analytical model [28]. Because most of the detected signal power is from a LoS path and the calculation of the corresponding path loss is simple, the light

propagation with only LoS transmission has been used in many VLC and LiFi studies. However, the detected signal power from non-line-of-sight (NLoS) paths has been found to be significant in certain scenarios [28], especially in small and reflective indoor environments. This NLoS channel is formed by a more complicated light propagation process. Most of the surrounding objects are not smooth relative to the wavelength of the optical signal. Consequently, the reflected optical signal is scattered, and this results in a countless number of reflected transmission paths, as shown in Fig. 2(b). In addition, the delay and attenuation of the signal via NLoS paths depends significantly on the characteristics of the specified indoor environment, such as room size, reflectance, and the properties of other objects. Many approaches have been proposed to simulate the responses of the NLoS channels [28,39]. In a widely used ray-tracing-based deterministic method, an empty cuboid room with six internal reflective surfaces (walls, floor, and ceiling) is assumed [28]. The surfaces are decomposed into small elements, and the light propagation interaction between each pair of surface elements is considered and evaluated. This approach can offer accurate NLoS channel response results, but the calculation is recursive and therefore time consuming. The calculation time is proportional to N^k, where N is the number of surface elements and k refers to the highest order of reflections. Consequently, the computational complexity increases prohibitively with the order of reflections. Practically, only simulations with $k \leq 3$ can be conducted. To improve the computation efficiency and flexibility, a number of variants have been proposed [39–41]. In particular, a Monte-Carlo-based method is able to generate a NLoS channel response within a few minutes with any order of reflections. This is considerably shorter than the computation time required for the deterministic method. However, the issue with this method is that an extra simulation error will be introduced. This means that the simulated channel impulse response fluctuates around the actual response (it either overestimates or underestimates the channel impulse response). The significance of this fluctuation is determined by a relative cumulative error. With a sufficiently large number of 500,000 rays, the relative cumulative error can be decreased to about 0.01 [42]. Recently, a frequency-domain calculation of the NLoS channel responses has been proposed [43], which converts the recursive operations into matrix inversion operations. Similar to the two methods mentioned above, this approach is able to deal with any indoor environment and transmitter/receiver configurations. By using the

Jacobi algorithm, the number of operations is proportional to kN^2. Therefore, the calculation time is significantly shortened compared to the deterministic method. In order to define the NLoS channel with a simpler model, a NLoS channel response expression based on a sphere physical model has been proposed, and the final expression interestingly is very simple [29]. However, it is found to be accurate in some indoor configurations but inaccurate in a number of others [43]. This is because it does not cater to the effects of the actual transmitter and receiver configurations. In order to improve the simulation accuracy, a method based on a commercial optical design tool, Zemax, has been proposed [44].

In several studies, special issues related to the VLC channel have been considered. For example, the VLC channel dependency on wavelength is considered [45]. A simple method is proposed to calculate the indoor free-space channel for a wide-spectrum VLC system. In addition, the shadowing effect is considered, which has been investigated in several initial studies [46–48]. It has been found that the impact of the human body mainly depends on the data rate, body reflectance, and receiver-to-body separation [47]. In [49], the authors show that random blockage events can be modeled by a Rayleigh distribution. It is also shown that angular diversity receivers referred to as "fly-eye receivers" [50] offer a good solution to link obstruction.

3. LIFI NETWORKS

LiFi falls under the larger umbrella of VLC. Much of VLC research focuses on point-to-point communication. Furthermore, most VLC research assumes that the visible light spectrum is used for both uplink and downlink communication. In contrast, LiFi encompasses broader networked systems, including multiuser, bidirectional, multicast, or broadcast communication. While it uses the visible light spectrum for downlink, LiFi uses the infrared spectrum for the uplink. LiFi is enabled by an ecosystem of multiuser techniques, resource allocation algorithms, and security strategies. These essential system components are illustrated in Fig. 3. LiFi networks were designed from the start to work seamlessly with RF wireless networks, e.g., Wi-Fi, to enable efficient, opportunistic load balancing, and augmented capacity in heterogeneous networks [51].
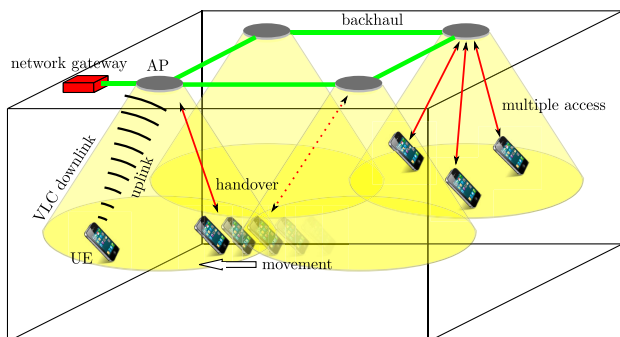
Fig. 3. LiFi network illustration. A complete LiFi network includes downlink, uplink, and backhaul connections. In addition, the system should provide a handover function, mobility support, and multiple access capability.

Moreover, a LiFi network includes multiple access points (APs) forming ultrasmall cellular networks to provide high-data-density wireless communication services to multiple mobile users simultaneously [20]. We use the terms "mobile users" and "user equipment" (UE) interchangeably. The LiFi network must support handover when users move across different light coverage regions.

In a LiFi network, a bidirectional connection between an AP and a UE is established whereby it is possible that an AP serves multiple users simultaneously. In addition, backhaul connections between APs and the network gateway are essential to enable AP cooperation and to establish a connection to the external network [52]. These backhaul connections can be provided by optical fiber, power-over-Ethernet, or powerline communications [52,53]. The LiFi downlink is piggy-backed on existing LED lighting systems. This is because LED lighting is becoming increasingly popular and it has been demonstrated that multi-Gbps transmission via LEDs is indeed possible [54]. In a LiFi network, an uplink connection is required for sending transmission acknowledgements, channel state information (CSI), and uploading files as well as enabling voice and video calls. Since using visible light in the uplink may cause distractions to the mobile user, the use of the infrared spectrum is deemed most appropriate for this link direction. This has the additional benefit that there is no interference between uplink and downlink and simultaneous communication can be established. Despite several initial studies on the infrared-based uplink [55,56], further comprehensive investigations in this direction are required. Furthermore, a number of RF-based communication technologies can also be considered, such as Bluetooth, ZigBee, or Wi-Fi [57]. These systems are readily available, but they may interfere with existing RF wireless systems. However, it has been reported that an RF/VLC hybrid communication system with VLC for downlink only is able to offload a significant amount of data traffic [58] and to exhibit low latency [59].

A complete LiFi network is composed of handover, multiple access, and co-channel interference (CCI) coordination, as shown in Fig. 3. There are two types of handover: horizontal handover and vertical handover. Horizontal handover refers to a change of the serving AP from within the same radio access technology (RAT). Vertical handover refers to a change of the serving AP belonging to a different RAT. For example, mobile users may be transferred from a LiFi AP to a Wi-Fi AP when none of the LiFi APs are able to offer a reliable link or the speed of the user is too high so that the dwell time in a cell is too short to establish a meaningful communication link. When the user slows down and enters the coverage of a lightly loaded LiFi AP, it may be best to handover to that LiFi AP to relieve the Wi-Fi network for more efficient operation (e.g., ensuring less packet collisions) [60]. An initial study on the horizontal handover scheme in LiFi networks has been carried out by Vegni [61]. In addition to the horizontal handover, vertical handover is also necessary to guarantee continuous connectivity. A vertical handover scheme based on the prediction of uncertainty metrics has been proposed by Shufei [62], which shows a significant reduction in transmission delays. Additionally, due to the smaller cell size and blockage issues

of LiFi networks, the frequency of handover increases significantly. Therefore, soft handover or handover skipping schemes have to be implemented [63]. Handover skipping refers to the techniques that enable handover between nonadjacent APs and omit APs causing unnecessary handovers. To improve the robustness of LiFi networks, fast link switching schemes with the use of pre-scanning and received signal strength (RSS) prediction have been proposed [64]. With the increased requirement on the capacity of wireless networks, dense spatial reuse of transmission resources is inevitable. Wireless links using the same transmission resource will interfere with each other. First, the users in adjacent cells may share the same transmission resource. In this case, the interference is known as CCI. In some cases, the same transmission resource is reused by users within the same cell. The interference between these users is known as intra-cell interference. Generally, intra-cell interference is handled by using orthogonal multiple access techniques. CCI is alleviated by appropriate interference coordination techniques. Interference coordination techniques will be discussed in Section 4.

Recently, the use of a cell-centric architecture to establish a multitier heterogeneous network to support extremely dense cells has been proposed [65,66]. The cell-centric approach dynamically adjusts the network topology based on user demand. For example, if there is no user within the coverage of a LiFi AP, this AP could turn off its communication functionality and only act as an ordinary lightbulb. This would mean that interference to neighboring cells is avoided. The motivation for the cell-centric approach in LiFi stems from the radical shrinkage of cell sizes to the range of 1 to 2 m in radius. Consequently, the load of an AP varies significantly in these systems [67]. Based on the user-centric architecture, the original cells centered at APs are turned into virtual cells centered on major clusters of users. This can be achieved by dynamically merging and disaggregating cells. In order to realize such user-centric architecture, user location must be known, and user positioning has been considered by Feng [68], for example. In addition to pursuing improved communication performance, enhanced energy efficiency has also been considered by Li [69].

To further boost the downlink transmission speed of LiFi networks, some research groups have considered optical wireless systems using one-directional coherent signal transmission in combination with very narrow beam steering. A recent study has reported potential link data rates of over 400 Gbps [70]. In a different study, a laser source with an optical diffuser is used, which is able to offer both illumination and wireless communication simultaneously [71]. In another design, centrally processed coherent optical signals are transmitted through optical fiber to an optical beam-steering system, which further directs the coherent signal via fixed grading structures to the target user wirelessly [72]. The uplink is achieved using RF systems. Several research groups have studied such alternative system designs using collimated beam steering to guarantee coverage that is different from LiFi networks using diffused beams [70,73,74]. However, beam-steering techniques could indeed further improve spatial reuse in LiFi networks, but this requires more work to overcome some practical limitations. For example, achieving user tracking with low complexity and high

reliability is challenging, especially when the LoS link is interrupted. Furthermore, optical fiber connections are required for high-speed backhaul connections, which increase installation complexity and cost. Furthermore, uniform lighting is not supported with these system designs.

4. INTERFERENCE COORDINATION TECHNIQUES

In order to boost the aggregate capacity of a LiFi network, dense spatial reuse of transmission resources is desirable. Consequently, inter-cell interference, or CCI, becomes a limiting factor that determines the overall performance of LiFi networks, as shown in Fig. 4(a). CCI in LiFi networks has been characterized [75]. In order to mitigate the negative effects of CCI, various interference mitigation techniques have been proposed [76–78].

The appropriate allocation of orthogonal transmission resources, such as time, space, frequency, and power, to users that contend for the same spectrum resource has been widely used in RF wireless cellular networks to achieve interference coordination. Several similar methods have also been considered in LiFi networks, including the additional wavelength dimension. One of the methods is known as static resource partitioning. In this method, the available transmission resources are split into multiple blocks. These resource blocks are assigned to the users in a fashion that adjacent APs always use different resource blocks, as shown in Fig. 4(b). The transmission resources can be split in either the time domain [76], the wavelength domain [79], or the frequency domain [80]. The assignment of these resource blocks is predefined, and the plan will not change during the operation of the LiFi system. This method can effectively avoid CCI with extremely low complexity. However, only a small fraction of the transmission resources can be used by each AP, which leads to significant reductions in system spectral efficiency [81]. An improved static resource partitioning method, known as fractional frequency reuse (FFR) [82], has been considered to mitigate the loss in spectral efficiency. In FFR, users are categorized as cell edge users and cell center users. All cell center users served by each AP share a single resource block as they experience low CCI, as shown in Fig. 4(c). Different resource blocks are assigned to the cell edge users served by adjacent APs in an orthogonal fashion to avoid CCI. By increasing the proportion of the resource assigned to the center users, the overall system spectral efficiency is improved due to an increase of the reuse rate of the transmission resources. Despite the simplicity of the fixed resource partitioning methods, they exhibit inefficiencies when the load of APs is uneven. In order to avoid such a loss of resource allocation efficiency, dynamic resource allocation schemes have been considered [81,83]. In one such study conducted by Ghimire, the transmission resources are split into multiple chunks in the time and frequency domains in an orthogonal frequency division multiple access time division duplex (TDD) optical wireless network deployed in an aircraft cabin [81]. Each UE broadcasts a signal of fixed power, which is a parameter that is known network wide. This simple power signal is transmitted in a mini-slot, which is referred to as a "busy burst" (BB). The BB protocol exploits channel
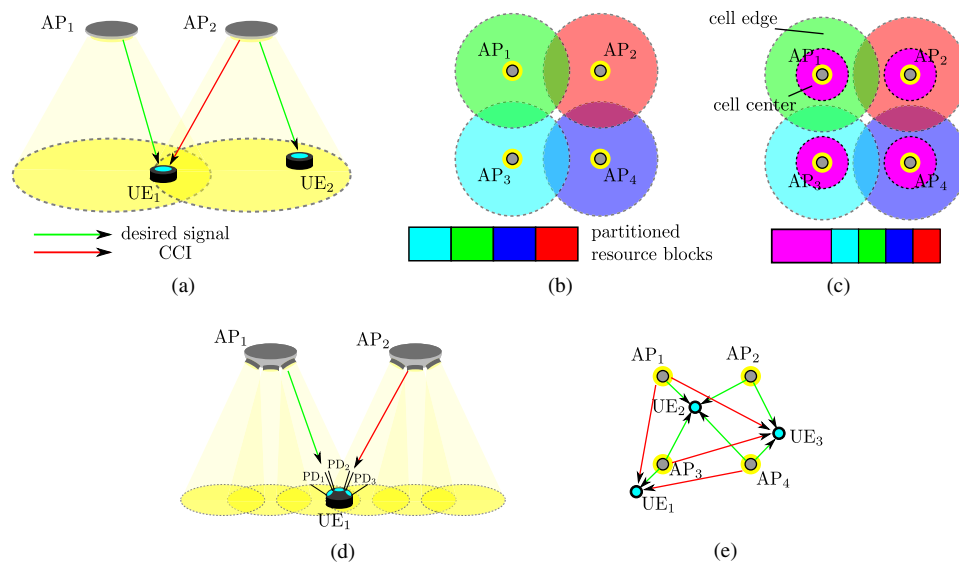
Fig. 4. (a) Demonstration of CCI. (b) Static resource partitioning. (c) Fractional frequency reuse. (d) Interference coordination with angular diversity transmitters and receivers. (e) Cooperative multipoint joint transmission.

reciprocity in TDD. The advantage of this scheme is that any potential interferer can estimate the interference it would cause based on the received BB signal power. The potential interferer can use this information to develop an appropriate transmission strategy. Based on this BB signaling, the resource chunks are dynamically allocated to UEs. It has been shown that the BB approach can significantly improve user fairness and the achievable spectral efficiency when compared to static resource allocation methods. Bykhovsky considers a time-division multiple access discrete multi-tone LiFi network with four APs and formulates the dynamic resource allocation as an optimization problem with a max–min criteria [83]. With appropriate simplifications, sub-optimal solutions of transmission power allocation and subcarrier scheduling can be obtained. Dynamic resource allocation schemes are able to adapt the allocation solution with the instantaneous AP load condition. However, it requires CSI at the AP side, and the computational complexity is higher than those of static resource partitioning approaches.

Apart from the methods borrowed from RF cellular techniques, unique approaches in LiFi networks exploiting angular diversity at both the transmitter and receiver side have also been considered [84]. On the receiver side, multiple PD detectors with small fields-of-view and different orientations can be mounted to function as an angular diversity receiver, as shown in Fig. 4(d). The desired signal from the tagged AP and the CCI from other adjacent APs may be incident to the receiver from different directions and are detected by different PD detectors. By using various combining techniques, the effect of CCI can be mitigated without loss of spectral efficiency. Using imaging receivers, it is also possible to achieve considerable spatial diversity to suppress CCI [85]. On the AP side, multiple light sources with narrow beamwidth can be mounted on the AP to form an angular diversity transmitter, as shown in Fig. 4(d). In such a system, the light source oriented to the desired UE is active [86]. Due to the narrow beamwidth, the spread of CCI is confined to a very limited area. The performance improvements stemming from interference coordination using angular diversity techniques come at the expense of increased hardware and algorithmic complexity.

Another promising interference mitigation approach is to coordinate transmissions from multiple APs so that a cell-edge user is served by multiple APs, as shown in Fig. 4(e). This is known as cooperative multipoint joint transmission (CoMP-JT) in RF wireless systems. However, this concept can be more easily deployed in a LiFi network, as there are no fast fading effects in IM/DD-based systems. In addition to the benefit of the elimination of CCI and enhancement of the desired signal, the possibility of blockage is lower due to the existence of multiple LoS transmission paths [67,87]. In particular, based on the concept of CoMP-JT, an improved user-centric vectored transmission technique with zero-forcing precoding has been proposed by Li to offer better bandwidth efficiency and flexibility [67]. On the other hand, CoMP-JT is based on coordination between adjacent APs, which requires centralized control.

5. LIFI NETWORK PERFORMANCE ANALYSIS

In this section, the performance of LiFi networks is considered and evaluated. This is extended to hybrid LiFi/Wi-Fi networks. Finally, we report results from a real-world hybrid LiFi/Wi-Fi network deployed in a school. With appropriate cooperation between the two networks, the overall system performance can be significantly improved as there is no mutual interference.

A. Capacity of Cellular LiFi Networks

The wireless capacity is an important system performance metric in a LiFi network. Shannon has proposed a channel capacity bound for a general communication link [88] assuming Gaussian signals and noise. In the case of IM/DD-based optical wireless systems, additional constraints on the optical
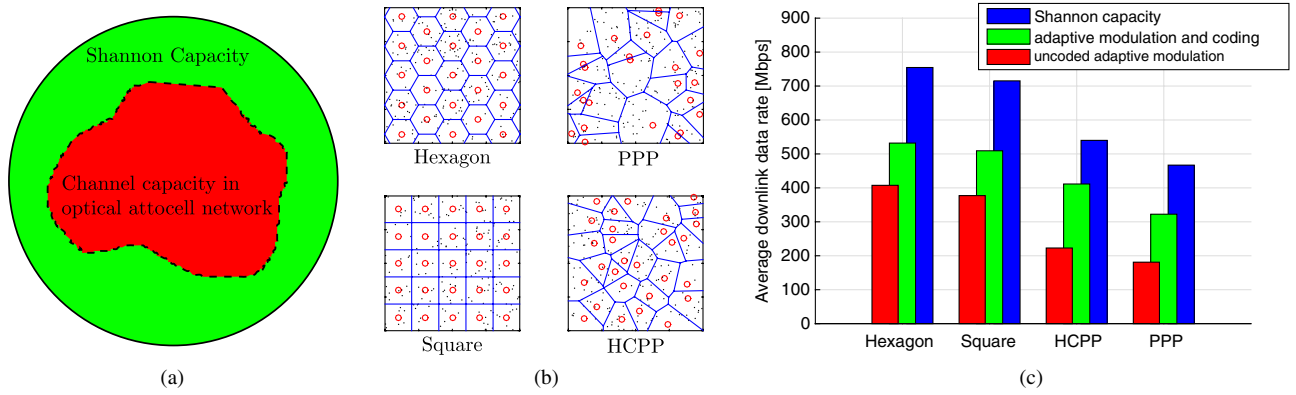
Fig. 5. (a) Relationship between Shannon capacity upper bound and channel capacity in a LiFi network. (b) Various cell layouts in LiFi networks. (c) Example of downlink performance in a LiFi network with an average cell radius of 2.5 m, and a source half-power semiangle of 40°.

transmission system are imposed, which suggest new capacity bounds for an optical link whose signals are constrained to be real-valued and nonnegative. A number of works have proposed more accurate capacity bounds of IM/DD-based optical wireless communication systems with average optical power and peak optical power constraints in the presence of noise [89,90]. In particular, Ma has considered the achievable data rate with a broadcast channel for two users with an average electrical power constraint [91]. However, these studies consider point-to-point links and only noise at the receiver. For the analysis of LiFi networks, we consider electrical signals at the receiver after optical-to-electrical conversions, which are bipolar, as well as considering the effect of CCI in the electrical domain. Therefore, we use the Shannon limit as an upper bound to estimate the channel capacity of a LiFi network. As illustrated in Fig. 5(a), it is recognized that there is a gap between the upper bound calculated by the Shannon–Hartley equation and the actual system capacity of a LiFi network.

However, this upper bound is instrumental in understanding trends and the fundamental relationships between system parameters and their impact on the achievable data rate. Therefore, we define an upper bound of a LiFi link as

$$c = \frac{1}{2} W \log_2 \left(1 + \frac{\sigma_0^2 \| H_0 \|^2}{\sum_{i \in I} \sigma_i^2 \| H_i \|^2 + W N_0} \right), \quad \textbf{(1)}$$

where W refers to the modulation bandwidth, σ_i^2 refers to the electrical signal variance from the ith AP, and $\| H_i \|^2$ refers to the channel gain from the ith AP to the desired user. I refers to the set of APs using the same transmission resource, thereby causing CCI, and N_0 is the double-sided noise power spectral density. In the case of $i = 0$, this corresponds to the serving AP. In Eq. (1), the rational term in the logarithm function corresponds to the electrical signal-to-interference-plus-noise ratio (SINR). The higher the SINR, the higher the achievable capacity. There are various ways to improve the SINR. By inspection of the SINR expression, an appropriate resource allocation is able to minimize the value of the CCI term $\sum_{i \in I} \sigma_i^2 \| H_i \|^2$. In addition, it is desirable to maximize the modulation bandwidth W outside the logarithm function. However, with an increase of W, the channel gain term $\| H_i \|^2$ decreases due to the front-end low-pass characteristics, and this also leads to

the increase of the noise term $W N_0$. Therefore, in order to use a large modulation bandwidth, front-end elements with high channel gain in the high-frequency region are required and transmission power from the tagged AP has to be sufficient.

As discussed in Section 2, the channel gain term $\| H_i \|^2$ does not only depend on the front-end elements, it also depends on the indoor free-space channel, which is related to the spatial distribution of APs. Chen has evaluated the downlink performance of LiFi networks studying various network deployments [21]. Hexagonal and Poisson point process (PPP) cell deployments have been used as the best and worst cases, respectively, in terms of CCI. This is because, on one hand, the separation between APs is maximized in the case of a hexagonal cellular layout, which confines the occurrences of strong CCI within a limited region at the cell edges. On the other hand, there is no constraint on the separation between APs in a PPP cellular layout. Therefore, the resulting CCI is much more pronounced. Under the assumption that the LiFi network is deployed on top of an existing lighting network, the spatial layout of lamps in a practical case is unlikely to follow an optimized hexagonal grid or indeed a completely random PPP layout. Consequently, we consider two additional AP topologies that emulate more closely practical deployments. One is a square-grid layout, and the second is a random layout following a hardcore point process (HCPP) [92], as shown in Fig. 5(b). The downlink performance of a LiFi network with various AP layouts is illustrated in Fig. 5(c). The presented results correspond to LiFi networks using spectral-efficient direct current optical OFDM modulation. The data rate calculation is based on a practical white LED [93]. The results show that the achievable average downlink data rate ranges from 180 to 530 Mbps, and the systems with hexagonal and PPP cell deployment offer the highest and lowest data rate, respectively. The data rate achieved by the square-grid network is slightly worse than that achieved by the hexagonal network. The data rate achieved by the HCPP network is higher than the PPP network but lower than the square-grid network.

The uplink in LiFi poses some extra challenges. First, the energy efficiency of the modulation technique is of key concern as the operation of mobile devices is constrained by batteries. Layered modulation techniques [94,95], therefore,

seem most appropriate as they enable almost zero direct current bias, which is a major energy consumer in high-speed IM/DD systems. Second, since the mobile terminal can take any orientation, directed transmission may yield significant signal-to-noise ratio (SNR) fluctuations. There have only been a few studies that focus on the uplink of LiFi networks [55,56]. The main principle used to develop robust uplink communication is based on spatial diversity. The effectiveness of spatial diversity has also been demonstrated in industrial environments where reliability is a key concern [96]. In a recent study it is shown that it is possible to develop an omni-directional transmitter for the uplink by considering transmitters on at least three sides of a mobile device [97].

B. Hybrid LiFi/Wi-Fi Networks and Load-Balancing Techniques

LiFi networks can be deployed to offload traffic from higher tier RF networks, such as Wi-Fi. Wi-Fi technology uses an inefficient carrier sensing multiple access scheme and has limited bandwidth. Within a large indoor area, the same spectrum cannot be reused at a similar density as the infrared and visible light spectrum. Consequently, the aggregate system throughput of Wi-Fi is limited, and the user data rate is low when there are too many active devices, as demonstrated in Fig. 6(a). In contrast, each LiFi AP can provide a high-speed wireless connection. However, strong blockages and fast UE movement/rotation may cause the connection between the UE and the LiFi AP to become unreliable in a LiFi standalone network, as demonstrated in Fig. 6(b). Therefore, the cooperation

between the Wi-Fi and LiFi networks could potentially alleviate the weaknesses of each system and improve the overall system performance [58], as shown in Fig. 6(c). In addition, the user-centric architecture proposed for future small-cell networks provides the convenience of implementing such cross-network-technology collaboration [67]. A prototype hybrid network has been reported by Ayyash [98], which achieves a significant improvement in the average system throughput.

Efficient load balancing in such a hybrid network is one of the main issues [99]. Based on the channel, user location, and speed as well as load conditions, the AP association and the allocation of transmission resources are adjusted to maximize a given objective function, as shown in Fig. 6(d). The load-balancing technique in a hybrid LiFi/Wi-Fi network aims at allocating the transmission resources of the LiFi and Wi-Fi systems jointly [100]. This forms a complicated optimization problem, and various methods have been studied to solve this. Wang has formulated the load-balancing challenge as a mixed-integer nonliner programming problem [101]. A joint optimization algorithm and a separate optimization algorithm have been proposed, which can find the optimum solution, but the computational complexity is large. Li has carried out another load-balancing optimization study in a VLC/Wi-Fi hybrid network, where the combined transmission and vectored transmission in the VLC network have been included [76]. However, the computational complexity is extremely high. In the follow-up study by Wang, a game-theory-based distributed approach has been proposed [102], which requires lower computational complexity but offers a solution that
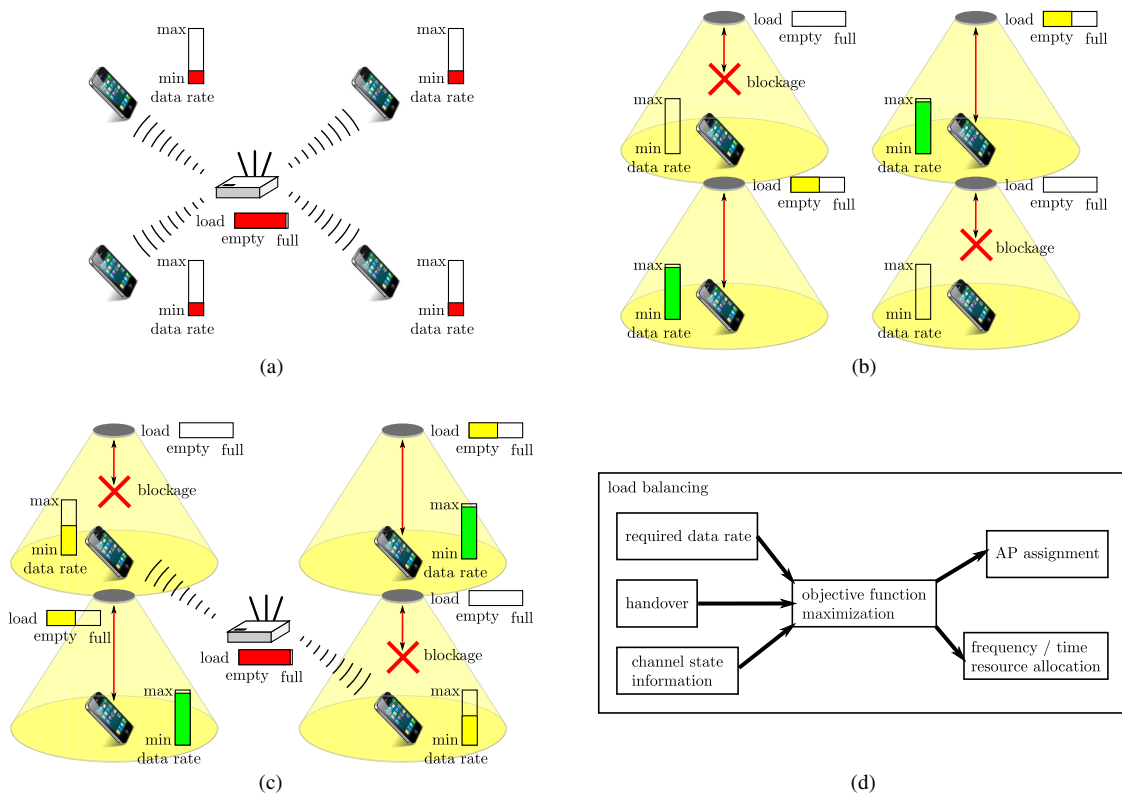
Fig. 6. (a) Wi-Fi standalone network. (b) LiFi standalone network. (c) LiFi/Wi-Fi hybrid network. (d) Load balancing in LiFi/Wi-Fi hybrid network.

is only asymptotic to the global optimum. This method is found to be very flexible in solving very complex cross-layer optimization problems. However, this heuristic approach has low tractability, which makes analytical evaluation and proof of optimality difficult. In recent studies, the load balancing in LiFi/Wi-Fi hybrid networks in dynamic conditions with UE movement and rotation is investigated [103]. It has been found that with optimal load-balancing solutions, the user quality of service can be improved by up to 80% compared to reported solutions [102]. Note that the quality of service refers to the user satisfaction level, which is defined as the ratio of the acquired data rate to the required data rate. In addition to maximizing the system communication performance, energy-efficient load balancing has also been considered. Kashef has carried out a study on the optimization of load balancing in an RF/VLC hybrid network in terms of energy efficiency [104]. It has been found that integrating LiFi in heterogeneous RF networks can significantly enhance energy efficiency, but more work is needed in this area.

C. LiFi Integration into a Hybrid LiFi/Wi-Fi Software Defined Networking Testbed

In order to facilitate the experimental validation of networking algorithms, such as handover, we have developed a testbed shown in Fig. 7. The testbed is composed of six LiFi attocells and a Wi-Fi AP. The APs are interconnected through a switch to a centralized software defined networking (SDN) OpenDaylight controller. This manages the SDN-enabled network through the southbound interface while supporting applications on its representational state transfer application program interface on the northbound. A LiFi access and traffic engineering application is running on top of the testbed, which supports network monitoring and management, user mobility, and network load balancing. The SDN controller has software agents running on the APs, which periodically send the state of APs to the controller. This exposes, in turn, the collected network state to the developed application to support the mentioned services.
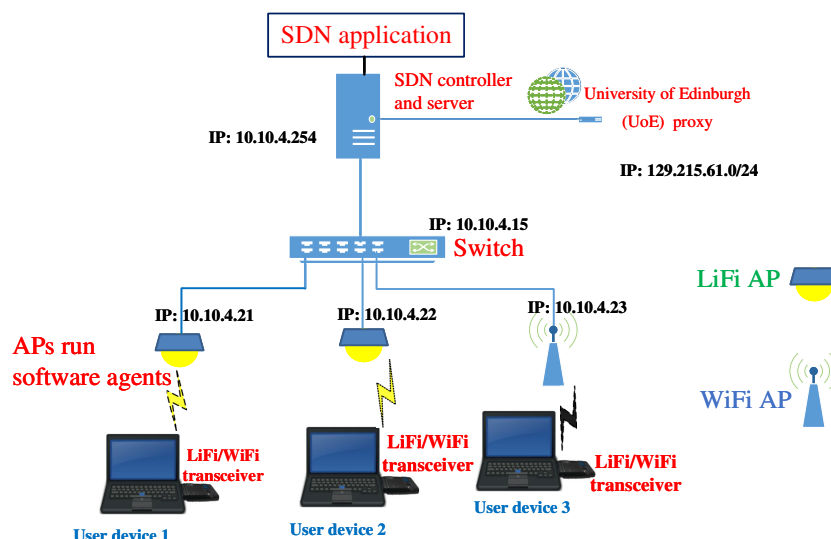
The testbed platform generates data relating to users, network, traffic flows, and supported services. As the testbed supports vertical handover between the heterogeneous LiFi and Wi-Fi networks, it is possible to trace the data flows of users during transitions from LiFi to LiFi and LiFi to Wi-Fi. An example of a horizontal and a vertical handover of a high-definition video service running on a mobile device is shown in Fig. 8. The mobile user slowly moves from the center of a LiFi AP to another LiFi AP, passing through the overlapping region. It then moves from the LiFi AP to the Wi-Fi AP.

This preliminary result shows that the time for horizontal handover is shorter than the time for vertical handover, as shown in Fig. 8. In both handover events the users experience short service disruption, which, however, is not noticeable as the service is running in a buffered mode.

In Fig. 9, the SNR is plotted when the user moves away from the center of the LiFi AP. The SNR is determined via system level simulations and measurements. The LiFi AP provides a high SNR around the cell center, which can be exploited to achieve very high data rates using adaptive modulation and coding techniques. It also shows the spatial confinement of the light signal, which can be harnessed to build ultradense wireless networks (within 1 m the SNR has dropped by 15 dB). In the next section, we provide results of a real-world LiFi network deployment in a school.

### D. Real-World Use Case: LiFi-Enabled Traffic Offloading in a Classroom

In this section we present the results of a real-world use case where a LiFi network was deployed in a classroom in addition to a Wi-Fi network. The network topology consists of eight LiFi attocell APs, as shown in Fig. 10. The LiFi attocell APs coexist with two additional Wi-Fi APs that serve seven classrooms. The Wi-Fi APs are commercially available and based on the IEEE 802.11ac standard. Each Wi-Fi AP can support data rates between 300 and 867 Mbps, depending on the mode of operation and bandwidth.

Fig. 7. Experimental SDN-enabled LiFi/Wi-Fi network testbed diagram, LiFi R&D Centre, UoE.
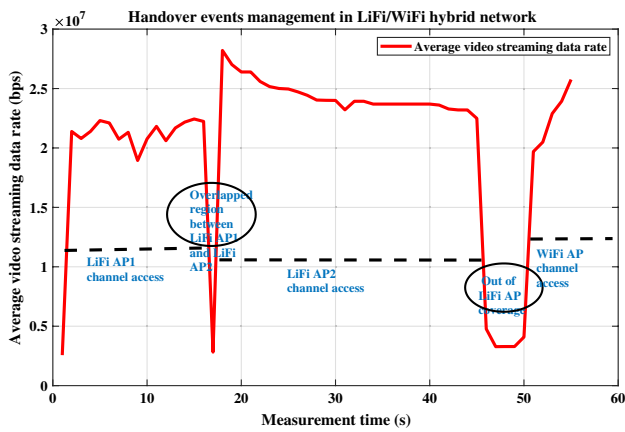
Fig. 8. Measured average data rate during handover of user device from LiFi to LiFi and LiFi to Wi-Fi.
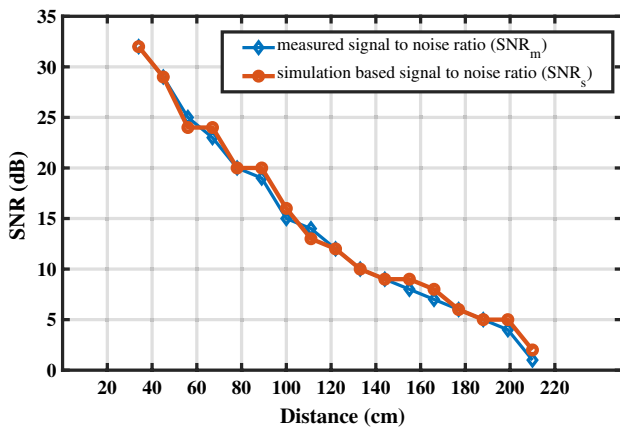
Fig. 9. Simulation-based and measured SNR under varying distance under a LiFi attocell.
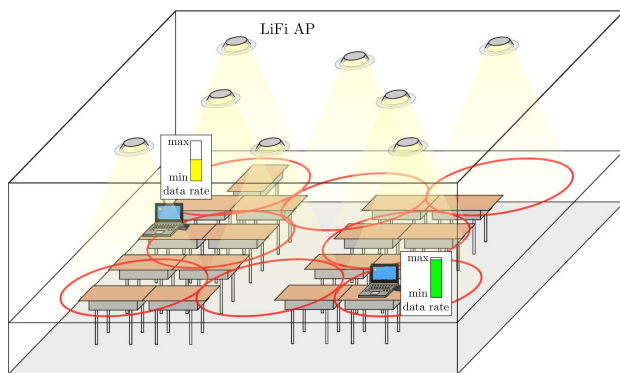
Fig. 10. Network topology of the LiFi APs in classroom 2 and the Wi-Fi AP serving both classrooms.

The Wi-Fi APs are deployed in the corridor of the school. As a result, typically a large number of users are served by each AP. This can lead to well-known throughput degradations because of MAC (medium access control) overheads as a result of contention resolution.

A commercially available LiFi system was deployed in a single classroom. Each LiFi AP can support a circular coverage area with diameters ranging between 2.8 and 3.5 m. The LiFi AP operates in full duplex mode and supports multiuser access and Internet protocol handover between the deployed APs. Each LiFi AP can support a maximum of eight users with a maximum aggregate data rate of 43 Mbps. This corresponds to a total maximum aggregated data rate of 344 Mbps per classroom. We note that the data rate of an access point is significantly lower than the VLC transmission speeds reported in lab experiments. The main reason is that this proof-of-concept system uses off-the-shelf unmodified LED luminaires whose electrical bandwidth is in the region of 2 MHz. The main purpose of this proof-of-concept demonstration in a real-world environment is to showcase the simultaneous functions of lighting and wireless networking using the same system. Future upgrades will include the integration of bespoke optical components within the luminaires leading to aggregate data performances of 1 and 10 Gbps. The latter will require bespoke luminaires, which are capable of wavelength division multiplexing.

The installation of the LiFi APs was constrained by the existing florescent lighting fixtures and the existing fire/smoke detector installation points. The LiFi luminaires were deployed alongside the existing infrastructure. As a result, there were some areas within the classroom that were not sufficiently covered by LiFi. Figure 10 shows the network setup. Therefore, the user performance is expected to be variable, depending on the user location. Ideally, the LiFi AP would replace the existing lighting infrastructure and would be optimized based on the room topology to provide the best trade-off between illumination and communication [105].

A measurement campaign was carried out with the aim to compare the performance of the LiFi and Wi-Fi networks and to assess the total aggregate data rate. The user data rate is used as a performance metric. A population of 22 pupils simultaneously accessed the LiFi network, and each of the two neighboring classrooms was served by Wi-Fi only. The pupil population in the neighboring classrooms was the same. Two tests were conducted based on unconstrained best effort data rates for different target data rates:

- a target data rate of 1 Mbps per user, and
- a target data rate of 3 Mbps per user.

The cumulative distribution function (CDF) of the user data rate achieved by the LiFi and Wi-Fi network is shown in Fig. 11 for the 1 and 3 Mbps data rate targets while in Fig. 12 the data rate without a target is reported. The results in Fig. 11 show that most of the users achieve the target data rate. However, some users fall short of the target data rate due to the suboptimum locations of the LiFi APs. Figure 12 demonstrates that there are some users in the LiFi network with considerably higher data rates up to 20 Mbps. It also shows that the user peak data rate is higher in the LiFi network despite the fact that the maximum data rate of the given LiFi AP is about 10 times lower than the maximum data rate of a deployed Wi-Fi AP. The average data rates for the LiFi and Wi-Fi networks are shown in Table 1. The results show that the LiFi network outperforms the Wi-Fi network in terms of "best-effort" average data rate,
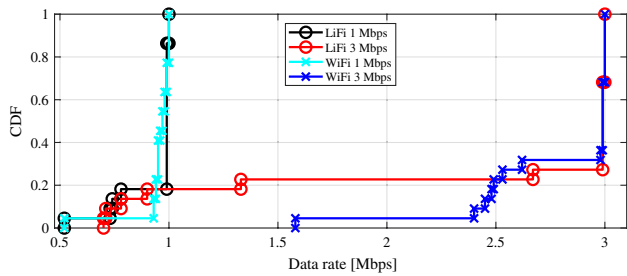
Fig. 11.   CDF of the data rate for the Wi-Fi and LiFi users based on the 1 Mbps and 3 Mbps data rate targets.
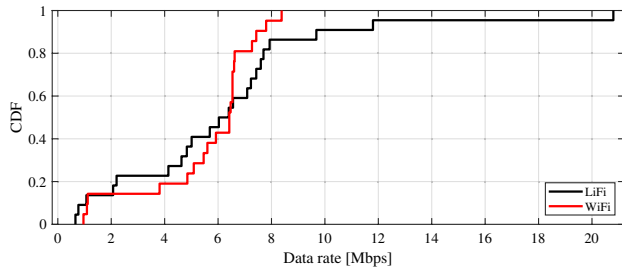
Fig. 12.   CDF of the data rate for the Wi-Fi and LiFi users assuming no data rate targets.

Table 1.   Average Data Rates Achieved for the Wi-Fi and LiFi Networks

Simulated User Target Data Rate	LiFi Users Average User Data Rate [Mbps]	Wi-Fi Users Average Data Rate [Mbps]
Best effort	6.24	5.57
1 Mbps	0.94	0.95
3 Mbps	2.50	2.79

as also shown in Fig. 12. However, the results also highlight that the LiFi network slightly underperforms compared to the Wi-Fi network at the targeted data rate of 3 Mbps. This is due to the low data rate achieved by the underperforming user equipment that is located at the LiFi attocell border regions and in dead-spot areas of the classroom.

An indirect but rather significant result of this proof-of-concept study was that there was a surge of the data rates in the neighboring Wi-Fi-only classrooms. This is because of the offload of data traffic to LiFi. Data rate gains in the neighboring classrooms are plotted in Fig. 13 for different target date rates.

This shows the capability of a LiFi network to offload traffic. This feature is particularly beneficial in dense environments like schools and airports. The results also demonstrate that frequency reuse gains are achievable within a small area—in this case a classroom. Our future work will aim to adopt the SDN-based dynamic load-balancing algorithms developed in the lab testbed described in Section 5 to real-world use cases, such as the LiFi network in a classroom.
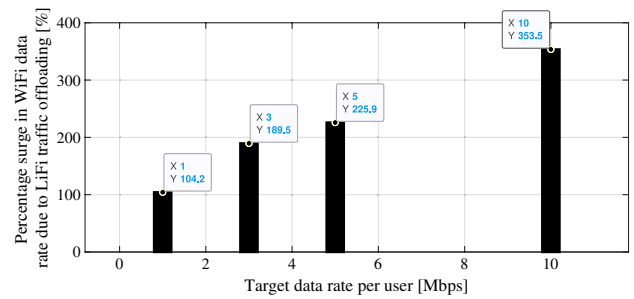
Fig. 13.   Surge in Wi-Fi aggregated data rate in neighboring classrooms.

6. CONCLUSIONS

This paper has shown that it is possible to build future cellular systems based on free-space light communication. In this context, it has highlighted that in order to achieve this objective, the focus in free-space light communications has to be shifted from point-to-point link-level data rate improvements in VLC to optimizing data densities in a wireless network. It was shown that LiFi can significantly improve Wi-Fi networks by offloading data traffic. This has the potential to extend data rates that are currently only possible in fiber-optic communication to the end users, which are, of course, our mobile devices. To achieve this vision, however, new optical devices would be required. In the meantime, this paper has shown that it is possible to enhance the data density significantly using LiFi in combination with Wi-Fi. This is because LiFi allows for step-change improvements in cell densification, enabling a radical reuse of transmission resources. This is an important feature due to the increasing number of devices that will need to be connected to the Internet. Mobile devices that define the beyond-smartphone era will require step-change improvements in the data rate, latency, and energy-efficiency, for example in augmented and virtual reality devices. However, there will be even more intelligent machine-type devices and a huge number of sensors in our future smart homes and smart cities, all of which will depend on reliable and high-speed wireless connectivity. In a commercial context, LiFi will enable the lighting industry to expand their business models into the telecommunications industry and vice versa. LiFi provides significant economic opportunities, but at the same time, there are many interesting scientific challenges to improve LiFi systems in order to fully leverage the vast amount of the unlicensed spectrum in the infrared and visible light domains.

REFERENCES

1. N. Zheludev, "The life and times of the LED—a 100-year history," Nat. Photonics **1**, 189–192 (2007).

2. T.-S. Chu and M. Gans, "High speed infrared local wireless communication," IEEE Commun. Mag. **25**(8), 4–10 (1987).

3. F. R. Gfeller and U. Bapst, "Wireless in-house data communication via diffuse infrared radiation," Proc. IEEE **67**, 1474–1486 (1979).

4. J. R. Barry, J. M. Kahn, E. A. Lee, and D. G. Messerschmitt, "High-speed nondirective optical communication for wireless networks," IEEE Netw. **5**, 44–54 (1991).

5. J. M. Kahn and J. R. Barry, "Wireless infrared communications," Proc. IEEE **85**, 265–298 (1997).

6. N. Holonyak, S. F. Bevacqua, C. V. Bielan, F. A. Carranti, B. G. Hess, and S. J. Lubowski, "Electrical properties of Ga(As1-xPx) p-n junctions," Proc. IEEE **51**, 364 (1963).

7. S. Nakamura, T. Mukai, and M. Senoh, "High-power GaN p-n junction blue-light-emitting diodes," Jpn. J. Appl. Phys. **30**, L1998–L2001 (1991).

8. H. Amano, M. Kito, K. Hiramatsu, and I. Akasaki, "p-type conduction in Mg-doped GaN treated with low-energy electron beam irradiation (LEEBI)," Jpn. J. Appl. Phys. **28**, L2112–L2114 (1989).

9. Y. Tanaka, T. Komine, S. Haruyama, and M. Nakagawa, "Indoor visible communication utilizing plural white LEDs as lighting," in *Proceedings of the 12th IEEE International Symposium on Personal, Indoor and Mobile Radio Communications* (2001), vol. **2**, pp. 81–85.

10. Y. Tanaka, S. Haruyama, and M. Nakagawa, "Wireless optical transmissions with white colored LED for wireless home links," in *Proceedings of the 12th IEEE International Symposium on Personal Indoor and Mobile Radio Communications (PIMRC)* (2000), vol. **2**, pp. 1325–1329.

11. J. Grubor, S. C. J. Lee, K. D. Langer, T. Koonen, and J. W. Walewski, "Wireless high-speed data transmission with phosphorescent white-light LEDs," in *Proceedings of the 33rd European Conference and Exhibition of Optical Communication—Post-Deadline Papers* (2007), pp. 1–2.

12. M. Z. Afgani, H. Haas, H. Elgala, and D. Knipp, "Visible light communication using OFDM," in *Proceedings of the IEEE 2nd International Conference on Testbeds and Research Infrastructures for the Development of Networks and Communities* (2006), pp. 129–134.

13. N. T. Le, M. S. Ifthekhar, Y. M. Jang, and N. Saha, "Survey on optical camera communications: challenges and opportunities," IET Optoelectron. **9**, 172–183 (2015).

14. M. Kinoshita, T. Yamazato, H. Okada, T. Fujii, S. Arai, T. Yendo, and K. Kamakura, "Motion modeling of mobile transmitter for image sensor based I2V-VLC, V2I-VLC, and V2V-VLC," in *IEEE Globecom Workshops (GC Wkshps)* (2014), pp. 450–455.

15. P. Luo, M. Zhang, Z. Ghassemlooy, H. Le Minh, H.-M. Tsai, X. Tang, L. C. Png, and D. Han, "Experimental demonstration of RGB LED-based optical camera communications," IEEE Photon. J. **7**, 7904212 (2015).

16. S. Cincotta, A. Neild, C. He, and J. Armstrong, "Visible light positioning using an aperture and a quadrant photodiode," in *IEEE Globecom Workshops (GC Wkshps)* (2017), pp. 1–6.

17. H. Steendam, T. Q. Wang, and J. Armstrong, "Theoretical lower bound for indoor visible light positioning using received signal strength measurements and an aperture-based receiver," J. Lightwave Technol. **35**, 309–319 (2017).

18. A. A. Al-Hameed, S. H. Younus, A. T. Hussein, M. T. Alresheed, and J. M. H. Elmirghani, "LiDAL: light detection and localization," IEEE Access **7**, 85645–85687 (2019).

19. B. Zhou, A. Liu, and V. Lau, "Joint user location and orientation estimation for visible light communication systems with unknown power emission," IEEE Trans. Wireless Commun. **18**, 5181–5195 (2019).

20. H. Haas, L. Yin, Y. Wang, and C. Chen, "What is LiFi?" J. Lightwave Technol. **34**, 1533–1544 (2016).

21. C. Chen, D. A. Basnayaka, and H. Haas, "Downlink performance of optical attocell networks," J. Lightwave Technol. **34**, 137–156 (2016).

22. Cisco Visual Networking Index, "Global mobile data traffic forecast update, 2017–2022," White Paper (2019), https://www.cisco.com/c/en/us/solutions/collateral/service-provider/visual-networking-index-vni/white-paper-c11-738429.html.

23. I. Stefan, H. Burchardt, and H. Haas, "Area spectral efficiency performance comparison between VLC and RF femtocell networks," in *IEEE International Conference on Communications (ICC)* (2013), pp. 3825–3829.

24. IEEE P802.11-Light Communication Task Group, "Status of IEEE 802.11 Light Communication TG" (2019), http://www.ieee802.org/11/Reports/tgbb_update.htm.

25. E. Calvanese Strinati, S. Barbarossa, J. L. Gonzalez-Jimenez, D. Ktenas, N. Cassiau, L. Maret, and C. Dehos, "6G: the next frontier: from holographic messaging to artificial intelligence using subterahertz and visible light communication," IEEE Veh. Technol. Mag. **14**(3), 42–50 (2019).

26. M. A. Khalighi and M. Uysal, "Survey on free space optical communication: a communication theory perspective," IEEE Commun. Surv. Tutorials **16**, 2231–2258 (2014).

27. H. Le Minh, D. O'Brien, G. Faulkner, L. Zeng, K. Lee, D. Jung, Y. Oh, and E. T. Won, "100-Mb/s NRZ visible light communications using a postequalized white LED," IEEE Photon. Technol. Lett. **21**, 1063–1065 (2009).

28. J. R. Barry, J. M. Kahn, W. J. Krause, E. A. Lee, and D. G. Messerschmitt, "Simulation of multipath impulse response for indoor wireless optical channels," IEEE J. Sel. Areas Commun. **11**, 367–379 (1993).

29. V. Jungnickel, V. Pohl, S. Nonnig, and C. von Helmolt, "A physical model of the wireless infrared communication channel," IEEE J. Sel. Areas Commun. **20**, 631–640 (2002).

30. E. Sarbazi, M. Uysal, M. Abdallah, and K. Qaraqe, "Indoor channel modelling and characterization for visible light communications," in *16th International Conference on Transparent Optical Networks (ICTON)* (2014), pp. 1–4.

31. M. Uysal, F. Miramirkhani, T. Baykas, and K. Qaraqe, "IEEE 802.11bb Reference Channel Models for Indoor Environments" (2018), https://www.researchgate.net/publication/327572598_IEEE_80211bb_Reference_Channel_Models_for_Indoor_Environments.

32. J. Vucic, C. Kottke, S. Nerreter, K. D. Langer, and J. W. Walewski, "513 Mbit/s visible light communications link based on DMT-modulation of a white LED," J. Lightwave Technol. **28**, 3512–3518 (2010).

33. L. Zeng, D. O'Brien, H. Le-Minh, K. Lee, D. Jung, and Y. Oh, "Improvement of date rate by using equalization in an indoor visible light communication system," in *4th IEEE International Conference on Circuits and Systems for Communications (ICCSC)* (2008), pp. 678–682.

34. J. J. D. McKendry, D. Massoubre, S. Zhang, B. R. Rae, R. P. Green, E. Gu, R. K. Henderson, A. E. Kelly, and M. D. Dawson, "Visible-light communications using a CMOS-controlled micro-light-emitting-diode array," J. Lightwave Technol. **30**, 61–67 (2012).

35. J. Ding, C.-L. I, and Z. Xu, "Indoor optical wireless channel characteristics with distinct source radiation patterns," IEEE Photon. J. **8**, 7900115 (2016).

36. H. Chen and Z. Xu, "OLED panel radiation pattern and its impact on VLC channel characteristics," IEEE Photon. J. **10**, 7901410 (2018).

37. F. Miramirkhani, O. Narmanlioglu, M. Uysal, and E. Panayirci, "A mobile channel model for VLC and application to adaptive system design," IEEE Commun. Lett. **21**, 1035–1038 (2017).

38. M. Uysal, F. Miramirkhani, O. Narmanlioglu, T. Baykas, and E. Panayirci, "IEEE 802.15.7r1 reference channel models for visible light communications," IEEE Commun. Mag. **55**(1), 212–217 (2017).

39. F. J. Lopez-Hernandez, R. Perez-Jimenez, and A. Santamaria, "Ray-tracing algorithms for fast calculation of the impulse response on diffuse IR-wireless indoor channels," Opt. Eng. **39**, 2775–2780 (2000).

40. J. B. Carruthers and P. Kannan, "Iterative site-based modeling for wireless infrared channels," IEEE Trans. Antennas Propag. **50**, 759–765 (2002).

41. F. J. Lopez-Hermandez and M. J. Betancor, "DUSTIN: algorithm for calculation of impulse response on IR wireless indoor channels," Electron. Lett. **33**, 1804–1806 (1997).

42. O. Gonzalez, S. Rodriguez, R. Perez-Jimenez, B. R. Mendoza, and A. Ayala, "Error analysis of the simulated impulse response on indoor wireless optical channels using a Monte Carlo-based ray-tracing algorithm," IEEE Trans. Commun. **53**, 124–130 (2005).

43. H. Schulze, "Frequency-domain simulation of the indoor wireless optical communication channel," IEEE Trans. Commun. **64**, 2551–2562 (2016).

44. F. Miramirkhani and M. Uysal, "Channel modeling and characterization for visible light communications," IEEE Photon. J. **7**, 1–16 (2015).

45. K. Lee, H. Park, and J. R. Barry, "Indoor channel characteristics for visible light communications," IEEE Commun. Lett. **15**, 217–219 (2011).

46. T. Komine and M. Nakagawa, "A study of shadowing on indoor visible-light wireless communication utilizing plural white LED lightings," in *Proceedings of the 1st International Symposium on Wireless Communication Systems* (2004), pp. 36–40.

47. C. Le Bas, S. Sahuguede, A. Julien-Vergonjanne, A. Behlouli, P. Combeau, and L. Aveneau, "Human body impact on mobile visible light communication link," in *Proceedings of the 10th International Symposium on Communication Systems, Networks and Digital Signal Processing (CSNDSP)* (2016), pp. 1–6.

48. Z. Dong, T. Shang, Y. Gao, and Q. Li, "Study on VLC channel modeling under random shadowing," IEEE Photon. J. **9**, 7908416 (2017).

49. P. Chvojka, S. Zvanovec, P. A. Haigh, and Z. Ghassemlooy, "Channel characteristics of visible light communications within dynamic indoor environment," J. Lightwave Technol. **33**, 1719–1725 (2015).

50. M. Kavehrad, M. I. S. Chowdhury, and Z. Zhou, "MIMO technology for optical wireless communications using LED arrays and fly-eye receivers," in *Short-Range Optical Wireless* (Wiley, 2015), pp. 169–191.

51. T. D. C. Little and M. Rahaim, "Network topologies for mixed RF-VLC HetNets," in *IEEE Summer Topicals Meeting Series (SUM)* (2015), pp. 163–164.

52. K. Chandra, R. V. Prasad, and I. Niemegeers, "An architectural framework for 5G indoor communications," in *International Wireless Communications and Mobile Computing Conference (IWCMC)* (2015), pp. 1144–1149.

53. H. Ma, L. Lampe, and S. Hranilovic, "Hybrid visible light and power line communication for indoor multiuser downlink," J. Opt. Commun. Netw. **9**, 635–647 (2017).

54. R. Bian, I. Tavakkolnia, and H. Haas, "15.73 Gb/s visible light communication with off-the-shelf LEDs," J. Lightwave Technol. **37**, 2418–2424 (2019).

55. M. T. Alresheedi, A. T. Hussein, and J. M. H. Elmirghani, "Uplink design in VLC systems with IR sources and beam steering," IET Commun. **11**, 311–317 (2017).

56. E. S. S. Edirisinghe, P. H. R. S. S. Karunarathna, D. M. T. B. Dissanayake, and G. M. R. I. Godaliyadda, "Design and implementation of a bi-directional visible light communication system," in *IEEE 10th International Conference on Industrial and Information Systems (ICIIS)* (2015), pp. 519–524.

57. P. Pérez-Nicoli, F. Silveira, X. Zhang, and A. Amara, "Uplink wireless transmission overview in bi-directional VLC systems," in *IEEE International Conference on Electronics, Circuits and Systems (ICECS)* (2016), pp. 588–591.

58. M. B. Rahaim, A. M. Vegni, and T. D. C. Little, "A hybrid radio frequency and broadcast visible light communication system," in *IEEE GLOBECOM Workshops* (2011), pp. 792–796.

59. S. Shao, A. Khreishah, M. B. Rahaim, H. Elgala, M. Ayyash, T. D. C. Little, and J. Wu, "An indoor hybrid WiFi-VLC Internet access system," in *IEEE 11th International Conference on Mobile Ad Hoc and Sensor Systems* (2014), pp. 569–574.

60. Y. Wang, S. Videv, and H. Haas, "Dynamic load balancing with handover in hybrid Li-Fi and Wi-Fi networks," in *IEEE 25th Annual International Symposium on Personal, Indoor, and Mobile Radio Communication (PIMRC)* (2014), pp. 548–552.

61. A. M. Vegni and T. D. C. Little, "Handover in VLC systems with cooperating mobile devices," in *International Conference on Computing, Networking and Communications (ICNC)* (2012), pp. 126–130.

62. S. Liang, H. Tian, B. Fan, and R. Bai, "A novel vertical handover algorithm in a hybrid visible light communication and LTE system," in *IEEE 82nd Vehicular Technology Conference (VTC2015-Fall)* (2015), pp. 1–5.

63. X. Wu and H. Haas, "Handover skipping for LiFi," IEEE Access **7**, 38369–38378 (2019).

64. T. Nguyen, M. Z. Chowdhury, and Y. M. Jang, "A novel link switching scheme using pre-scanning and RSS prediction in visible light communication networks," EURASIP J. Wireless Commun. Netw. **2013**, 293 (2013).

65. F. Boccardi, R. W. Heath, A. Lozano, T. L. Marzetta, and P. Popovski, "Five disruptive technology directions for 5G," IEEE Commun. Mag. **52**(2), 74–80 (2014).

66. R. Zhang, J. Wang, Z. Wang, Z. Xu, C. Zhao, and L. Hanzo, "Visible light communications in heterogeneous networks: paving the way for user-centric design," IEEE Wireless Commun. **22**, 8–16 (2015).

67. X. Li, F. Jin, R. Zhang, J. Wang, Z. Xu, and L. Hanzo, "Users first: user-centric cluster formation for interference-mitigation in visible-light networks," IEEE Trans. Wireless Commun. **15**, 39–53 (2016).

68. S. Feng, X. Li, R. Zhang, M. Jiang, and L. Hanzo, "Hybrid positioning aided amorphous-cell assisted user-centric visible light downlink techniques," IEEE Access **4**, 2705–2713 (2016).

69. X. Li, Y. Huo, R. Zhang, and L. Hanzo, "User-centric visible light communications for energy-efficient scalable video streaming," IEEE Trans. Green Commun. Netw. **1**, 59–73 (2017).

70. A. Gomez, K. Shi, C. Quintana, R. Maher, G. Faulkner, P. Bayvel, B. C. Thomsen, and D. O'Brien, "Design and demonstration of a 400 Gb/s indoor optical wireless communications link," J. Lightwave Technol. **34**, 5332–5339 (2016).

71. F. Zafar, M. Bakaul, and R. Parthiban, "Laser-diode-based visible light communication: toward gigabit class communication," IEEE Commun. Mag. **55**(2), 144–151 (2017).

72. K. Wang, A. Nirmalathas, C. Lim, and E. Skafidas, "4 × 12.5 Gb/s WDM optical wireless communication system for indoor applications," J. Lightwave Technol. **29**, 1988–1996 (2011).

73. T. Koonen, J. Oh, K. Mekonnen, and E. Tangdiongga, "Ultra-high capacity indoor optical wireless communication using steered pencil beams," in *International Topical Meeting on Microwave Photonics (MWP)* (2015), pp. 1–4.

74. A. T. Hussein, M. T. Alresheedi, and J. M. H. Elmirghani, "20 Gb/s mobile indoor visible light communication system employing beam steering and computer generated holograms," J. Lightwave Technol. **33**, 5242–5260 (2015).

75. M. Rahaim and T. D. C. Little, "Optical interference analysis in visible light communication networks," in *IEEE International Conference on Communication Workshop (ICCW)* (2015), pp. 1410–1415.

76. X. Li, R. Zhang, and L. Hanzo, "Cooperative load balancing in hybrid visible light communications and WiFi," IEEE Trans. Commun. **63**, 1319–1329 (2015).

77. A. A. Qidan, M. Morales-Cespedes, and A. G. Armada, "The role of WiFi in LiFi hybrid networks based on blind interference alignment," in *IEEE 87th Vehicular Technology Conference (VTC Spring)* (2018), pp. 1–5.

78. D. Miras, L. Maret, M. Maman, M. Laugeois, X. Popon, and D. Ktenas, "A high data rate LiFi integrated system with inter-cell interference management," in *IEEE Wireless Communications and Networking Conference (WCNC)* (2018), pp. 1–6.

79. K. Cui, J. Quan, and Z. Xu, "Performance of indoor optical femtocell by visible light communication," Opt. Commun. **298-299**, 59–66 (2013).

80. H.-S. Kim, D.-R. Kim, S.-H. Yang, Y.-H. Son, and S.-K. Han, "Inter-cell interference mitigation and indoor positioning system based on carrier allocation visible light communication," in *5th International Conference on Signal Processing and Communication Systems (ICSPCS)* (2011), pp. 1–7.

81. B. Ghimire and H. Haas, "Self-organising interference coordination in optical wireless networks," EURASIP J. Wirel. Commun. Netw. **2012**, 131 (2012).

82. C. Chen, S. Videv, D. Tsonev, and H. Haas, "Fractional frequency reuse in DCO-OFDM-based optical attocell networks," J. Lightwave Technol. **33**, 3986–4000 (2015).

83. D. Bykhovsky and S. Arnon, "Multiple access resource allocation in visible light communication systems," J. Lightwave Technol. **32**, 1594–1600 (2014).

84. K.-H. Park and M.-S. Alouini, "Optimization of an angle-aided mirror diversity receiver for indoor MIMO-VLC systems," in *IEEE Global Communications Conference (GLOBECOM)* (2016), pp. 1–6.

85. O. González, M. F. Guerra-Medina, I. R. Martín, F. Delgado, and R. Pérez-Jiménez, "Adaptive WHTS-assisted SDMA-OFDM scheme for fair resource allocation in multi-user visible light communications," J. Opt. Commun. Netw. **8**, 427–440 (2016).

86. Z. Chen, D. A. Basnayaka, and H. Haas, "Space division multiple access for optical attocell network using angle diversity transmitters," J. Lightwave Technol. **35**, 2118–2131 (2017).

87. R. Bai, H. Tian, B. Fan, and S. Liang, "Coordinated transmission based interference mitigation in VLC network," in *IEEE 82nd Vehicular Technology Conference (VTC2015-Fall)* (2015), pp. 1–5.

88. C. E. Shannon, "A mathematical theory of communication," Bell Syst. Tech. J. **27**, 379–656 (1948).

89. A. Lapidoth, S. M. Moser, and M. A. Wigger, "On the capacity of free-space optical intensity channels," IEEE Trans. Inf. Theory **55**, 4449–4461 (2009).

90. A. Chaaban, Z. Rezki, and M. S. Alouini, "On the capacity of the intensity-modulation direct-detection optical broadcast channel," IEEE Trans. Wireless Commun. **15**, 3114–3130 (2016).

91. S. Ma, R. Yang, H. Li, Z. L. Dong, H. Gu, and S. Li, "Achievable rate with closed-form for SISO channel and broadcast channel in visible light communication networks," J. Lightwave Technol. **35**, 2778–2787 (2017).

92. J. G. Andrews, F. Baccelli, and R. K. Ganti, "A tractable approach to coverage and rate in cellular networks," IEEE Trans. Commun. **59**, 3122–3134 (2011).

93. A. M. Khalid, G. Cossu, R. Corsini, P. Choudhury, and E. Ciaramella, "1-Gb/s transmission over a phosphorescent white LED by using rate-adaptive discrete multitone modulation," IEEE Photon. J. **4**, 1465–1473 (2012).

94. H. Elgala and T. D. C. Little, "SEE-OFDM: spectral and energy efficient OFDM for optical IM/DD systems," in *IEEE 25th Annual International Symposium on Personal, Indoor, and Mobile Radio Communication (PIMRC)* (2014), pp. 851–855.

95. Q. Wang, B. Song, B. Corcoran, D. Boland, L. Zhuang, Y. Xie, A. J. Lowery, A. J. Lowery, and A. J. Lowery, "FPGA-based layered/enhanced ACO-OFDM transmitter," in *Optical Fiber Communication Conference* (2017), paper Tu3D.6.

96. P. W. Berenguer, P. Hellwig, D. Schulz, J. Hilt, G. Kleinpeter, J. K. Fischer, and V. Jungnickel, "Real-time optical wireless communication: field-trial in an industrial production environment," in *European Conference on Optical Communication (ECOC)* (2018), pp. 1–3.

97. C. Chen, R. Bian, and H. Haas, "Omnidirectional transmitter and receiver design for wireless infrared uplink transmission in LiFi," in *IEEE International Conference on Communications Workshops (ICC Workshops)* (2018), pp. 1–6.

98. M. Ayyash, H. Elgala, A. Khreishah, V. Jungnickel, T. Little, S. Shao, M. Rahaim, D. Schulz, J. Hilt, and R. Freund, "Coexistence of WiFi and LiFi toward 5G: concepts, opportunities, and challenges," IEEE Commun. Mag. **54**(2), 64–71 (2016).

99. W. Ma and L. Zhang, "QoE-driven optimized load balancing design for hybrid LiFi and WiFi networks," IEEE Commun. Lett. **22**, 2354–2357 (2018).

100. M. Obeed, A. M. Salhab, S. A. Zummo, and M.-S. Alouini, "Joint optimization of power allocation and load balancing for hybrid VLC/RF networks," J. Opt. Commun. Netw. **10**, 553–562 (2018).

101. Y. Wang, D. A. Basnayaka, X. Wu, and H. Haas, "Optimization of load balancing in hybrid LiFi/RF networks," IEEE Trans. Commun. **65**, 1708–1720 (2017).

102. Y. Wang, X. Wu, and H. Haas, "Load balancing game with shadowing effect for indoor hybrid LiFi/RF networks," IEEE Trans. Wireless Commun. **16**, 2366–2378 (2017).

103. Y. Wang and H. Haas, "Dynamic load balancing with handover in hybrid Li-Fi and Wi-Fi networks," J. Lightwave Technol. **33**, 4671–4682 (2015).

104. M. Kashef, M. Ismail, M. Abdallah, K. A. Qaraqe, and E. Serpedin, "Energy efficient resource allocation for mixed RF/VLC heterogeneous wireless networks," IEEE J. Sel. Areas Commun. **34**, 883–893 (2016).

105. I. Stefan and H. Haas, "Analysis of optimal placement of LED arrays for visible light communication," in *IEEE 77th Vehicular Technology Conference (VTC Spring)* (2013).